Analysis of Rotational Resonance Magnetization Exchange Curves from Crystalline Peptides

Olve B. Peersen,[†,‡] Michel Groesbeek,[†] Saburo Aimoto,[§] and Steven O. Smith*[,†]

Contribution from the Department of Molecular Biophysics and Biochemistry, Yale University, New Haven, Connecticut 06520-8114, and Institute for Protein Research, Osaka University, Osaka 565, Japan

Received January 26, 1995[⊗]

Abstract: Rotational resonance is a solid-state NMR method for restoring homonuclear dipolar couplings in magic angle spinning (MAS) experiments. Measurements of dipolar couplings can be used to determine internuclear distances which in turn provide direct constraints on molecular structure. The dipolar coupling between two spins is estimated from the observed intensity changes in a magnetization exchange experiment carried out while spinning the sample at a rotational resonance condition, i.e. when $\Delta = n\omega_r$, where Δ is the difference in chemical shift of two dipole-coupled spins, ω_r is the rotational frequency in the MAS experiment, and n is a small integer corresponding to the rotational resonance order. Rotational resonance NMR data and calculations are presented for a crystalline 11-residue peptide incorporating pairs of ^{13}C labels separated by 3.7, 4.5, 4.8, 5.1, and 6.8 Å. We discuss the critical parameters in generating and interpreting the magnetization exchange curves that are used to relate the observed intensity changes in the rotational resonance spectra to dipolar couplings. The accuracy of internuclear distance estimates from these experiments depends on the precision of the measurements as well as correctly accounting for natural abundance background signals, the effects of proton B_1 field strengths, and inhomogeneous broadening of the dipole-coupled NMR resonances. For the crystalline 11-residue peptide, the precision and accuracy of the RR distance measurements are on the order of 0.1 and 0.2−0.3 Å, respectively. On the basis of these studies, we outline approaches for determining internuclear distances in both crystalline and non-crystalline solid-state samples.

Introduction

Rotational resonance (RR) is one of several solid-state NMR methods that have been developed recently for measuring dipolar couplings in magic angle spinning (MAS) NMR experiments.[1−3] These methods offer enormous potential for structural studies of polycrystalline and membrane-bound proteins since magic-angle spinning yields high resolution NMR spectra of these systems, and the measured dipolar couplings can be directly related to internuclear distances. A few selected distance measurements can be used to establish the local secondary structure along or the tertiary contacts between polypeptide chains, and thereby provide high resolution constraints on global protein structure.

Rotational resonance reintroduces the dipolar couplings in magic-angle spinning experiments when the rotational frequency of the sample matches a rotational resonance condition, $\Delta = n\omega_r$, where Δ is the difference in chemical shift within a magnetically isolated pair of two dipole coupled spins, ω_r is the sample rotation frequency in the MAS experiment, and n is a small integer corresponding to the rotational resonance order.[4] In order to measure the dipolar coupling and thereby determine the distance between two spins, one of the resonances in the spin pair is selectively inverted and the intensity of both resonances is monitored as a function of a mixing time during which magnetization is exchanged within the spin pair.[1,2] The observed intensity changes are expressed in a magnetization exchange curve which plots the integrated intensities of the resonances as a function of the mixing time. The *precision* in the RR NMR measurements depends on the sensitivity and the stability of the experiment, while the *accuracy* of the distances determined from the observed intensity changes depends on the experimental precision of the measurements as well as the approach taken to evaluate the magnetization exchange curves.

There are two approaches that have been taken to relate the magnetization exchange curves to internuclear distances. The first approach involves a direct comparison of the exchange curves for an unknown distance with curves obtained from crystalline model compounds where internuclear distances are known independently from a crystal structure.[5] We have previously shown that RR measurements can be used to examine $^{13}C\cdots{}^{13}C$ distances of 3.7−6.8 Å within an 11-residue crystalline peptide.[5] The undecapeptide, which models the N-terminus of alamethicin, was shown to adopt a helical structure in membranes by comparing exchange curves obtained from crystalline peptides with those from membrane-bound peptides. The second approach for determining internuclear distances involves simulating the observed RR data with theoretically calculated exchange curves.[2] In this paper, we extend our studies on the crystalline alamethicin peptides with calculations of the RR magnetization exchange curves based on geometrical parameters taken from the known crystal structure. By comparing data from five homologous $^{13}C\cdots{}^{13}C$ spin pairs that span a range of internuclear distances, we are able to explore the key parameters in the calculations and thus critically evaluate the accuracy and precision of RR-based distance determinations. These studies

[†] Yale University.

[‡] Current address: Department of Chemistry and Biochemistry, University of Colorado, Box 215, Boulder, CO 80309-0215.

[§] Osaka University.

[⊗] Abstract published in *Advance ACS Abstracts,* June 15, 1995.

(1) Raleigh, D. P.; Levitt, M. H.; Griffin, R. G. *Chem. Phys. Lett.* **1988**, *146*, 71.

(2) Levitt, M. H.; Raleigh, D. P.; Creuzet, F.; Griffin, R. G. *J. Chem. Phys.* **1990**, *92*, 6347.

(3) Gullion, T.; Schaefer, J. *Adv. Magn. Reson.* **1989**, *13*, 57. Hing, A. W.; Vega, S.; Schaefer, J. *J. Magn. Reson.* **1992**, *96*, 205. Tycko, R.; Smith, S. O. *J. Chem. Phys.* **1993**, *98*, 932.

(4) Andrew, E. R.; Bradbury, A.; Eades, R. G. *Nature* **1958**, *182*, 1659.

(5) Peersen, O. B.; Yoshimura, S.; Hojo, H.; Aimoto, S.; Smith, S. O. *J. Am. Chem. Soc.* **1992**, *114*, 4332.

0002-7863/95/1517-7228$09.00/0

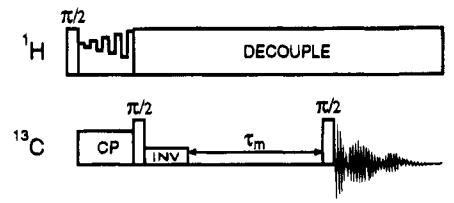

Figure 1. Pulse sequence for RR NMR. ^{13}C magnetization is generated in the $x-y$ plane using variable-amplitude cross polarization.[7] The magnetization is then stored along the z-axis with a flip-back pulse and one of the two dipole-coupled resonances is inverted using a low-power selective pulse. The magnetization is allowed to exchange during a variable mixing time and then returned to the $x-y$ plane for observation with a 90° pulse.

provide the foundation for evaluating RR NMR measurements of membrane-bound proteins and peptides.

Experimental Details

Sample Preparation. The 11-residue alamethicin peptides were synthesized as described previously.[5] Crystalline samples of the model peptides were grown by evaporation of methanol solutions. The internuclear distances between ^{13}C pairs in the undecapeptide are well-determined. We have previously solved the crystal structure of the undecapeptide grown from methanol solutions[5] and found that the rms difference between this structure and an earlier structure[6] grown from dichloromethane and diethyl ether was 0.08 Å for all atoms in the first five residues of the peptide where the ^{13}C labels are located and 0.11 Å overall. The double ^{13}C labeled peptides were diluted 1:5 with unlabeled peptide prior to crystallization to isolate the ^{13}C···^{13}C spin pairs in the crystal lattice and eliminate intermolecular magnetization exchange in the RR experiments. The 3.7-Å sample was crystallized at a final ratio of 1:1.6 to reduce the acquisition time for several control experiments. Data from this sample are identical to data from a 1:5 ratio sample, as is expected because in the crystal lattice there are no intermolecular distances closer than 10 Å between these two ^{13}C labeled nuclei and the RR exchange will thus be dominated by intramolecular exchange.[13]

Data Acquisition and Processing. All experiments were carried out on a Chemagnetics (Fort Collins, CO) CMX-360 spectrometer using a high-speed 5-mm probe made by Doty Scientific (Columbia, SC). The RF frequencies were 359.429 and 90.388 MHz for the ^{1}H and ^{13}C channels, respectively, and 90° pulse lengths were typically 3 and 4 μs. Cross polarization was accomplished using variable-amplitude cross polarization (VACP) with a 5-ms 11-amplitude contact time at a ^{13}C field strength of ~55 kHz. VACP improves signal intensity and stability at the high MAS rates required for the RR experiments.[7,8] The acquisition dwell time was 33.3 μs and the pulse repetition delay was 2.5 s. The RR pulse sequence is depicted in Figure 1.

The ^{13}C carrier frequency was placed in the middle of the spectrum (~110 ppm from TMS). All cross polarization and 90° pulses were at this frequency. The carbonyl resonance was selectively inverted with a 500-μs low-power pulse applied at a frequency offset of ~6 kHz from the carrier, resulting in a ~2 kHz wide excitation that fully inverted the resonances in the carbonyl region. The carbonyl resonance, rather than the methyl resonance, was inverted because there are few other resonances in this region of the spectrum whose intensities would be distorted by lying on the edges of the excitation spectrum. As a result, the entire methyl and methylene regions of the spectrum are unaffected by the inversion pulse and intensity changes in these regions can be used to assess both the selectivity of the RR exchange experiment and the contribution of any other relaxation pathways active during the RR mixing period.

The acquisition order of the different RR mixing times was randomized and the data were typically collected in 6 additive blocks, each of which constitutes a complete set of 32 different mixing times. For each mixing time, a total of 768 FIDs were collected. The MAS speed was controlled to within ±5 Hz with a computer based speed controller (Doty Scientific, Columbia, SC). The accuracy and response time of this controller is much better than that of an earlier controller home built from the design by De Groot *et al.*[9] and used for the previously published RR data collected on a 200-MHz spectrometer.[5]

The NMR data were processed with 15-Hz exponential line broadening, and a second or third degree polynomial baseline correction was made to the spectra after Fourier transformation and phasing. Resonance intensities in the RR spectra were evaluated by integrating the spectra. The chemical shift axis in the peptide spectra was referenced by setting the sharp resonance of the t-Boc quaternary carbon to 81.3 ppm from TMS.[6]

Exchange Curve Calculations. The parameters needed to simulate the RR data from the five crystalline peptides, listed in Table 1, were either obtained experimentally, taken from the literature, or derived from the crystal structure of the peptide. The isotropic chemical shifts of the ^{13}C-labeled carbonyl and methyl resonances were obtained from the background corrected spectra shown in Figure 2. The chemical shift anisotropy and asymmetry parameters were taken from the carbonyl tensor data obtained by Hartzell *et al*,[10] giving an anisotropy of 117.6 ppm (10630 Hz at 90.4 MHz) with an asymmetry parameter of 0.85, and the methyl group parameters were taken from alanine,[11] giving an anisotropy of 18.5 ppm (1672 Hz) and an asymmetry parameter of 0.32.

The relative orientations of the chemical shift and dipolar tensors are expressed in a set of Euler angles (α, β, γ) that specifies the rotations necessary to transform each tensor into a common crystal reference frame obtained from the known X-ray structure of the peptide. A computer program was written that calculates the Euler angles in two axis system transformations. First the principal axis system (PAS) of each chemical shift tensor is transformed into the local atomic molecular axis system. The orientation of the PAS relative to the local molecular structure must be known to perform this transformation. For the carbonyl tensor, the σ_{11} and σ_{22} elements are in the plane of the peptide bond with σ_{22} being almost colinear with the C=O bond and σ_{11} making a ~40° angle with the C−N peptide bond.[10,12] The orientation of the alanine methyl tensor was taken from Mehring.[12] For this spin only the σ_{33} tensor element can be specified exactly; it lies along the C_3 molecular axis of the methyl group which in alanine is the $C_\beta-C_\alpha$ bond. The other two elements are perpendicular to the axis, but their rotation about the C_3 axis can only be specified if the methyl group is attached to a plane of symmetry, in which case the σ_{11} element is perpendicular to this plane. The alanine residue does not contain a suitable symmetry plane and as a result the program was written such that the σ_{11} element is perpendicular to the plane formed by the alanine C_β, C_α, and C=O carbon atoms. This arbitrary rotation of the σ_{11} and σ_{22} elements will have minimal impact on the RR simulations because the methyl tensor is close to being axially symmetric. In the second transformation, the two spin tensors are rotated into the crystal axis system that is common to the entire structure. It is here that the X-ray crystal structure of the peptide is considered because it specifies the relative orientations of the two sets of molecular axis systems. This transformation cannot be performed without knowledge of the three-dimensional structure of the molecule. The program also calculates the Euler angles needed to rotate the dipolar tensor into the same common crystal axis system. The strength of the dipole coupling is calculated from the internuclear distance obtained from the X-ray crystal structure of the peptide.

The actual sample spinning speed used in the calculations was the average spinning speed observed during the data acquisition. Typical experimental deviations were ±5 Hz, which do not affect the simulations. Spinning about the magic angle was assumed and 1000 different

(6) Schmitt, H.; Winter, W.; Bosch, R.; Jung, G. *Liebigs Ann. Chem.* **1982**, *1982*, 1304. Bosch, R.; Jung, G.; Schmitt, H.; Winter, W. *Biopolymers* **1985**, *24*, 961−978.
(7) Peersen, O. B.; Wu, X.; Kustanovich, I.; Smith, S. O. *J. Magn. Reson.* **1993**, *104*, 334.
(8) Peersen, O. B.; Wu, X.; Smith, S. O. *J. Magn. Reson.* **1994**, *106*, 127.
(9) De Groot, H. J. M.; Copié, V.; Smith, S. O.; Allen, P. J.; Winkel, C.; Lugtenburg, J.; Herzfeld, J.; Griffin, R. G. *J. Magn. Reson.* **1988**, *77*, 251.
(10) Hartzell, C. J.; Whitfield, M.; Oas, T. G.; Drobny, G. P. *J. Am. Chem. Soc.* **1987**, *109*, 5966.
(11) Duncan, D. *J. Phys. Chem. Ref. Data* **1987**, *16*, 125.
(12) Mehring, M. *Principles of high-resolution NMR in solids*; Springer-Verlag: Berlin, 1988.
(13) Peersen, O. B. Ph.D. Thesis, Yale University, 1994.

Table 1. Parameters Used for the RR Simulations of the Five Crystalline Peptides[a]

	3.7 Å	4.5 Å	4.8 Å	5.1 Å	6.8 Å
carbonyl					
isotropic shift (Hz)	3962	4065	3911	3911	3999
anisotropy (Hz)	10630	10630	10630	10630	10630
asymmetry	0.85	0.85	0.85	0.85	0.85
orientation (α, β, γ)	89, 76, 157	119, 97, 113	40, 112, 142	40, 112, 142	3, 116, 125
methyl					
isotropic shift (Hz)	−10451	−10451	−10465	−10326	−10333
anisotropy (Hz)	1672	1672	1672	1672	1672
asymmetry	0.32	0.32	0.32	0.32	0.32
orientation (α, β, γ)	17, 98, 134	17, 98, 134	17, 98, 134	119, 34, 1	119, 34, 1
dipole					
coupling (Hz)	151	84.0	67.6	56.6	24.7
orientation (α, β, γ)	0, 55, 0	0, 48, 0	0, 19, 0	0, 94, 0	0, 148, 0
MAS rate (Hz)	14413	14516	14376	14237	14332

[a] The orientations are expressed in Euler angles relative to the axis coordinate system of the X-ray structure. The spinning axis was set to 54.736°, all J couplings were set to zero, and the powder averaging was done with 1000 crystallites over the orientation range $0° \leq \alpha \leq 360°$ and $0° \leq \beta \leq 180°$.

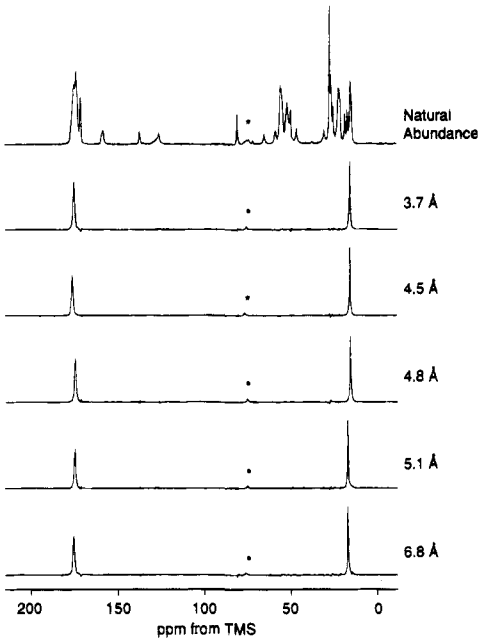

Figure 2. The natural abundance ^{13}C spectrum of the crystalline undecapeptide (top) and difference spectra showing the isotopically labeled ^{13}C resonances in each of the five peptides. All spectra were obtained and processed under identical conditions of 9 kHz MAS and 83 kHz proton decoupling. Optimal subtractions were obtained by scaling and shifting the natural abundance spectrum relative to the spectra of the five ^{13}C labeled peptides so as to minimize the difference spectrum in regions where isotopically labeled resonances or spinning sidebands are not present.

crystallite orientations were averaged. Several calculations, the results of which are not shown, were performed to establish to what extent the theoretically predicted transfer curves depend on the values of the input parameters. The exchange curves varied by at most 0.05 units of $\langle I_{zs} - I_{z1} \rangle$ in response to changing the tensor asymmetry from 0.0 to 1.0, changing the carbonyl anisotropy from 5 to 15 kHz, or changing the methyl anisotropy from 0.4 to 3.0 kHz. Therefore, small errors in the tensor input parameters do not influence the conclusions in this work.

Generation of RR Magnetization Exchange Curves

Difference Spectroscopy and the Assignment of ^{13}C-Labeled Resonances. The isotropic chemical shifts of the isotopically labeled ^{13}C sites were determined by difference spectroscopy (Figure 2); VACP MAS spectra of crystalline unlabeled and the five diluted ^{13}C labeled peptide samples were obtained under identical conditions. The natural abundance spectrum was subtracted from the spectrum of each diluted labeled peptide to yield a spectrum with only the resonances from the two ^{13}C-labeled sites. The spectra were obtained at 9 kHz MAS to average the chemical shift anisotropy of most ^{13}C nuclei in the sample while minimizing the spectral overlap of the isotropic centerband and any remaining spinning sidebands. At this spinning speed, which corresponds to 100 ppm, only the carbonyl resonance at 175 ppm has significant spinning sidebands (marked with asterisks). The resonances in the difference spectra were numerically fit to Lorentzian line shapes and the resulting parameters are listed in Table 2. These show excellent agreement between different peptides sharing a single labeling site; for example, both the 4.8- and 5.1-Å peptides use the carbonyl of Ala_1 and the fitted values of the two resonance positions and widths differ by only 1.6 and 3.0 Hz, respectively. The average widths observed for the carbonyl and methyl resonances are 80.9 and 35.8 Hz, respectively.

Background Signal Quantitation. The natural abundance background signals can directly affect the *apparent* amount of RR magnetization exchange. This can be a severe problem for carbon studies with overlapping resonances in the carbonyl, methylene, and methyl regions of the spectrum. As an example, consider a RR experiment where background signals account for one-half of the intensity found in an unresolved carbonyl resonance. If an experiment is carried out in which the labeled nuclei exchange by 50%, then the overall intensity of the entire unresolved carbonyl resonance will change by only 25% because the labeled nuclei constitute half of the initial intensity. The observed magnetization exchange rate then appears smaller than the real rate and the internuclear distance will be overestimated. Consequently, it is important to accurately subtract the contribution of background signals in the RR exchange spectra prior to normalizing the exchange curve to the initial intensity of the labeled spin pair.

The method used here is to determine the contribution of background signals by integrating the difference spectra shown in Figure 2 in parallel with the spectra of the ^{13}C-labeled peptides to calculate the percentage of the observed intensity that is due to the ^{13}C labels and to natural abundance background (Table 2). The background signals were quantitated in this way for three different regions of the spectra: two regions extending ±2.5 ppm from the isotropic chemical shifts of the two ^{13}C labels in each peptide, and a third region encompassing only the CH and CH_2 resonances (43−62 ppm). An estimate of the accuracy of the subtractions can be made by considering the background in this latter region (data not shown), which is

Table 2. Lorentzian Line Shape Parameters Obtained from the Difference Spectra Shown in Figure 2[a]

	^{13}C carbonyl			^{13}C methyl		
distance, Å	position, Hz	width, Hz	background, %	position	width	background, %
3.7	−3970.3	78.8 ± 1.8	27.5	10444	45.2 ± 1.1	18.0
4.5	−4073.9	80.4 ± 1.6	33.9	10448	32.3 ± 0.5	28.7
4.8	−3923.3	81.5 ± 1.6	38.1	10461	35.6 ± 0.3	26.4
5.1	−3921.8	78.5 ± 1.5	40.2	10327	31.0 ± 0.6	27.8
6.8	−4003.5	85.4 ± 1.7	40.0	10329	34.7 ± 0.6	29.0
average	n/a	80.9 ± 1.6	n/a	n/a	35.8 ± 0.6	n/a

[a] The line widths have been corrected for the 15 Hz line broadening applied during data processing. Background signals were quantitated as described in the text based on regions ±2.5 ppm from the isotropic resonances.

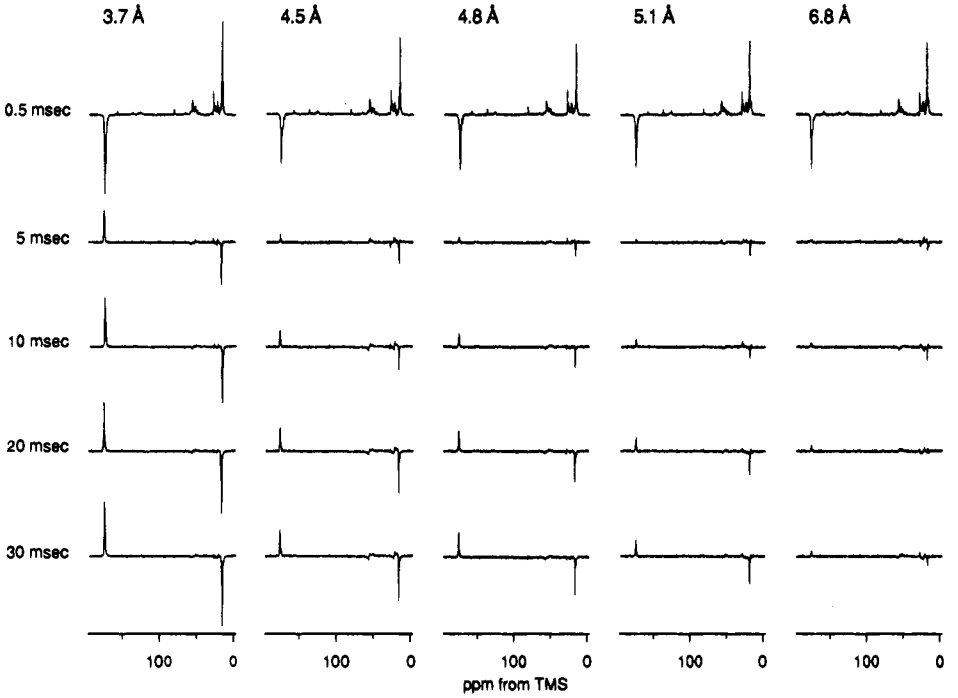

Figure 3. RR difference spectra showing the extent of magnetization exchange in the five ^{13}C-labeled peptides. The top spectra were acquired with a RR mixing time of 0.5 ms and the additional spectra reflect only the changes in these spectra as the mixing period is increased. Spectra were acquired at the $n = 1$ RR condition using VACP and 83 kHz proton decoupling the mixing and acquisition periods.

devoid of ^{13}C labels and should contain 100% natural abundance background signals. The average observed value of 102.6% argues that the background signal percentages are accurate to within 2−3%. In the RR experiments, the average signal intensity observed from the first four mixing times (0.1, 0.5, 0.75, and 1.0 ms) was used to get an accurate measure of the full initial intensity (i.e. labeled + background). The magnitude of the background signals was then determined by multiplying through by the percentages given in Table 2, and this fixed background signal was then subtracted from each time point in the RR exchange data set prior to any other processing of the RR data.

RR Magnetization Exchange Spectra. Figure 3 shows $n = 1$ RR magnetization exchange difference spectra of the five crystalline peptides generated by subtracting a short mixing time spectrum (0.5 ms) from spectra obtained with longer mixing times. Only the two exchanging resonances are present because signals from non-exchanging spins cancel out in the subtraction. Large intensity changes are observed for the 3.7-Å peptide reflecting the strong dipolar coupling between the two ^{13}C labels. Small, but measurable, intensity changes are observed for the 6.8-Å peptide. The 6.8-Å distance represents an upper limit for ^{13}C···^{13}C RR NMR distance measurements.

Close examination of these difference spectra reveals an apparent splitting due to the restoration of the homonuclear ^{13}C···^{13}C dipolar coupling under RR conditions. As shown by

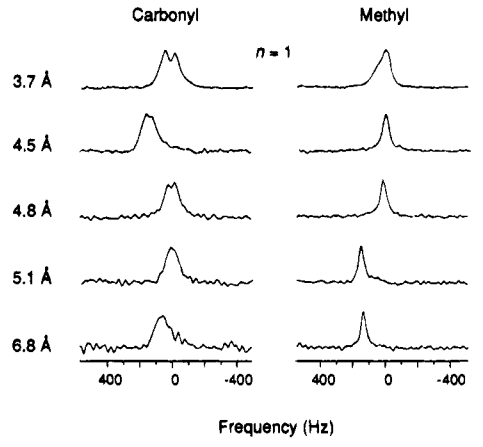

Figure 4. RR difference spectra showing the line shapes of the exchanging portion of the carbonyl and methyl resonances in the $n = 1$ experiments of the five peptides. The spectra were obtained by subtracting spectra with 2 and 28 ms mixing times, and all resonances are shown as positive peaks for clarity.

the expanded plots in Figure 4, the carbonyl splitting appears to depend on the internuclear distance, being most pronounced for the 3.7-Å peptide and decreasing with increasing distance to the point where it is not readily visible in the spectrum from the 6.8-Å peptide. The splitting is independent of the decoupling field strength used during the RR and acquisition periods[13] and

Table 3. RR-Induced Splittings of the ^{13}C Carbonyl and Methyl Resonances[a,b]

distance, Å	dipolar coupling (Hz)	proton decoupling (kHz)	^{13}C carbonyl (Hz)	^{13}C methyl (Hz)
3.7	151	83	69.6 ± 0.6	46.3 ± 2.2
		70	65.2 ± 0.4	
		60	67.7 ± 0.6	
		50	65.7 ± 2.8	
		62[d]	69.5 ± 3.3	
4.5	84	83	45.3 ± 1.9	c
4.8	68	83	49.1 ± 2.1	
5.1	57	83	40.9 ± 3.6	
6.8	24	83		

[a] Results obtained at 90.4 MHz unless otherwise noted. [b] The resonances were fit to Lorentzian line shapes. [c] Line splittings were not observed. [d] Data obtained at 50.3 MHz.[5]

is also independent of the static magnetic field strength, as shown by $n = 1$ RR difference spectra obtained from earlier work[5] at a lower field strength (4.7 T) where the $n = 1$ spinning speed was only 8020 Hz. The observed RR induced splittings were quantitated by line fitting of the difference spectra (Table 3). The carbonyl resonances could be fit to two lines (except for the 6.8-Å data). However, for the methyl resonances, only the resonance from the 3.7-Å peptide could be justifiably fit to two lines, indicating that the splittings are not symmetric for the two members of the rotationally coupled $^{13}C\cdots{}^{13}C$ spin pair. The remaining four methyl resonances do, however, exhibit reduced line width as a function of the internuclear distance.

The observed splittings have the potential of providing direct information on the dipolar couplings *without* undertaking a magnetization exchange experiment. However, the line shape effects depend on the orientation of the chemical shift tensors and are still not well understood for small couplings in the presence of large anisotropies.[2] The splittings are not symmetric on the carbonyl and methyl resonances, as would be expected based on previous ^{13}C RR spectra and line shape simulations of zinc acetate.[1,2] Furthermore, line shape simulations based on the couplings and molecular geometry of the crystalline peptides predict line splittings of only ~35 Hz for the 3.7-Å peptide and slight line broadening without observable splittings for the other four peptides (data not shown).

RR Magnetization Exchange Curves. Interpretation of the raw intensity changes observed in the RR experiment requires the generation of a magnetization exchange curve which is a normalized plot of the intensity distribution of the two exchanging resonances as a function of the mixing time. The intensity distribution was calculated as the difference of the background corrected intensities (vide supra), $I[CH_3] - I[C{=}O]$, where the $I[C{=}O]$ intensity is negative. The exchange data were then normalized to an initial value of 1.0 by dividing through by the average of the first four mixing time points. The resulting exchange curves obtained with 62- and 83-kHz proton decoupling during the RR mixing time are shown in Figure 5.

The steepest decay in Figure 5 is observed for the 3.7-Å peptide and the magnetization exchange curve reveals a dipolar oscillation. The oscillation becomes damped when the proton decoupling strength is reduced to 62 kHz, as discussed in more detail below. The 4.5, 4.8, and 5.1 Å ^{13}C spin pairs all exhibit non-oscillatory RR exchange curves with both 62- and 83-kHz proton-decoupling strengths and the order of their decay rates is as expected from their internuclear distances. The 6.8-Å peptide shows only a slight decay as a function of the mixing time and the decay rate does not change substantially with decreased proton decoupling. The high *precision* in the

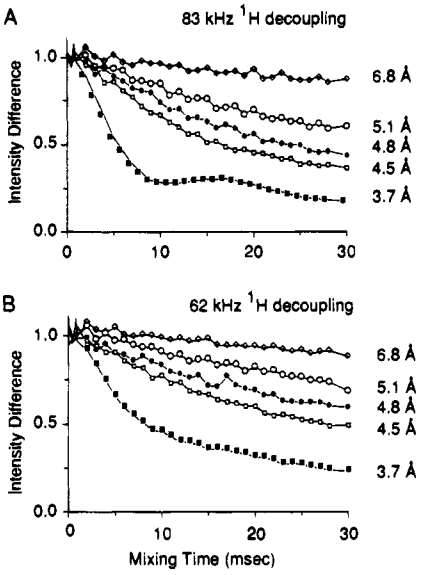

Figure 5. $n = 1$ RR exchange curves obtained from the five alaminiscule peptides with 83 and 62 kHz proton decoupling during the RR mixing period. The internuclear distances are indicated on the plot. The curves were generated by subtracting an experimentally-determined natural abundance background signal before calculating the intensity difference ($I[CH_3] - I[C{=}O]$) and normalizing the curves to an initial value of 1.0 by averaging the data from the first four time points.

measurements as reflected by the low scatter in the experimental points results mainly from high sensitivity, interleaving of data acquisition, and stability in cross polarization using the variable-amplitude CP sequence. The experimental resolution of these data is on the order of 0.1 Å based on the clear differences between the exchange curves from the three middle distances, which pairwise differ from each other by 0.3 Å.

Dependence of Magnetization Exchange on Spinning Speed and Decoupling. The requirement for accurate spinning speed control is demonstrated with exchange data from the 3.7 and 6.8 Å spin pairs. The data shown in Figure 6A compare the 6.8 Å exchange curve observed at the exact $n = 1$ RR condition with 83- and 62-kHz proton decoupling to the curve observed where the sample is spinning 332 Hz below the $n = 1$ RR condition. The off-RR decay of intensity is primarily due to T_1 relaxation. Linear fits to the initial slope of the exchange curves show a clear difference between the on- and off-RR rates. Figure 6B presents a plot of the slope of the initial part of the 3.7 Å exchange curve (2−10 ms) as the MAS rate is swept through the $n = 1$ RR condition. These data show a sharp spinning speed dependence that can be numerically fit to a Lorentzian line shape with a full width at half height of 200 Hz. Focusing on the peak of this fit, it is apparent that spinning speed control within ± 15 Hz of the exact RR condition is required to get maximum exchange rates.

The decoupling dependence of magnetization exchange is expanded upon for the 3.7 Å $^{13}C\cdots{}^{13}C$ spin pair in Figure 7A. These data show that incomplete proton decoupling prevents magnetization exchange between the coupled spins, resulting in loss of the oscillation in the 3.7 Å exchange curve. The exchange curves obtained with a 83, 70, and 60 kHz decoupling strength come together at an "isosbestic" or merge point at ~20 ms as the dipolar oscillation is damped out. The presence of such a merge point is predicted by the simulations.[2] The 50 kHz decoupling data do not reach this point because the transfer rate has become too slow.

In practice, the dependence of the observed exchange rate on decoupling is also complicated by the non-uniform distribu-

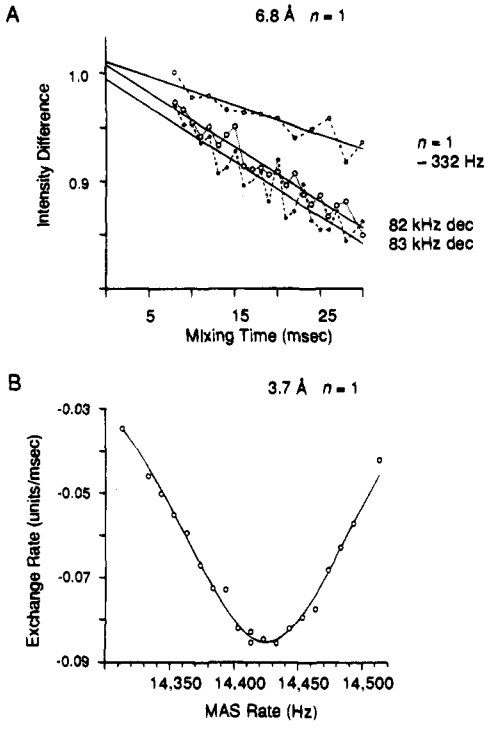

Figure 6. (A) Comparison of on and off $n = 1$ exchange rates in the 6.8-Å peptide. The lines are linear fits to the data between 7 and 30 ms. The early time points were excluded because of large scatter in the data that adversely affected the linear interpolation (see Figure 8). (B) Spinning speed dependence of RR exchange in the 3.7-Å peptide. The plot is of the linear slope of the initial part of the exchange curve (2−10 ms) versus the MAS rate. The line fit is to a Lorentzian line centered at 14425 ± 0.9 Hz with a full width at half maximum of 209.3 ± 20 Hz.

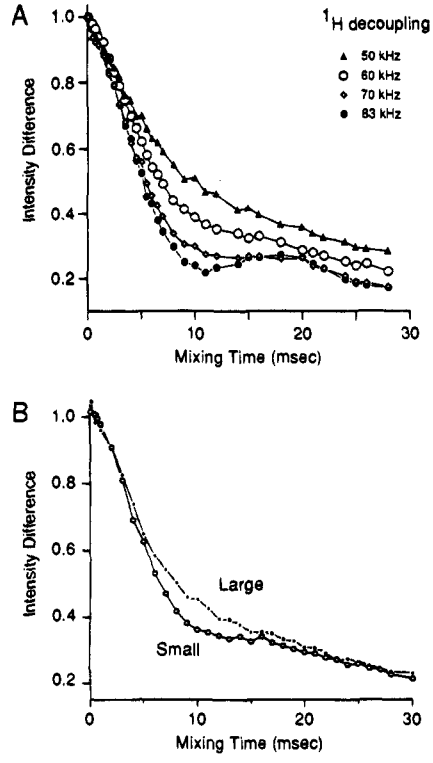

Figure 7. Decoupling strength and sample size dependence of the RR exchange rates in the 3.7-Å peptide. (A) The proton decoupling field strength was changed as indicated and the data were processed as in Figure 5. The sample filled the full length of the rotor. (B) 62 kHz decoupling curves showing RR curves obtained with the sample filling the rotor (large) or repacked into only the central 3.5 mm of the rotor (small).

tion of decoupling strengths across the sample due to B_1 field inhomogeneity in the probe coil. It is well-known that the strength of the B_1 magnetic fields generated by RF pulses is subject to inhomogeneity effects in the sample coil.[8,14] The effect is that as the sample volume is increased, the effective decoupling field is decreased on portions of the sample and the observed magnetization exchange curve is damped (Figure 7B).

Simulations of the Experimental Magnetization Exchange Curves

In an effort to establish the accuracy and resolution of RR distances determined by calculations, we have used the theoretical treatment described by Levitt *et al.*[2] to predict the exchange curves of the crystalline peptides. In using this treatment to derive dipolar couplings, particular attention must be paid to the zero-quantum relaxation time parameter which has a strong effect on the RR exchange rates. The zero-quantum relaxation time (T_2^{ZQ}) is a measure of the lifetime of the transverse coherence of the pair of coupled spins during the RR mixing period.[2] Several relaxation and experimental factors can be accounted for by this term, including residual proton couplings not removed by RF decoupling, homonuclear flip−flop interactions with other spins, and effects of local motions. These factors interfere with the coherent exchange of Zeeman magnetization between the dipole-coupled spins.

RR Magnetization Exchange Calculations. We have carried out RR exchange calculations using a number of different T_2^{ZQ} values to determine whether the data from all five model peptides could be fit with a common zero-quantum relaxation time. Such a comparison is feasible because the internuclear distances are known and fixed for the five peptides so that the strength of the homonuclear dipolar coupling is not a free parameter. The zero-quantum relaxation rates are likely to be equal in all five peptides because the five distances involve identical pairs of backbone carbonyl and alanine methyl atoms and the data were obtained under identical experimental conditions. The residual proton couplings that are not removed by proton decoupling should be the same for the five peptides since to a first approximation the groups and their environments are the same. Moreover, the peptide molecules are fixed in a crystal lattice with little freedom for local molecular motions that can selectively average nuclear interactions for some spin pairs but not for others.

The plots in Figure 8 compare the calculated and observed RR exchange curves obtained from the five peptides with 62 and 83 kHz proton decoupling. Simulations using T_2^{ZQ} values ranging from 1.0 to 3.5 ms in 0.5-ms steps are shown. The optimal zero-quantum relaxation times needed to predict the data from the 3.7, 4.5, 4.8, and 5.1 Å $^{13}C\cdots^{13}C$ spin pairs are 1.5−2.0 ms for the 62 kHz proton decoupling data and 3.0−3.5 ms for 83 kHz decoupling data. It is clear from these plots that the sensitivity of the RR exchange curves to the proton decoupling strength can be accounted for by changing the zero-quantum relaxation time used in the simulations; reduced proton decoupling strength requires a reduced T_2^{ZQ} value. More importantly, the data from the four different peptides can indeed be simulated using a common value for the T_2^{ZQ}.

The calculations are not as conclusive for the 6.8-Å data because the RR exchange rates are inherently slow due to the weak (25 Hz) dipolar coupling between the ^{13}C spins. These

(14) Idziak. S.: Haeberlen. U. *J. Magn. Reson.* **1982**, *50*, 281.
(15) Kubo. A.: McDowell. C. A. *J. Chem. Soc., Faraday Trans. 1* **1988**, *84*, 3713.

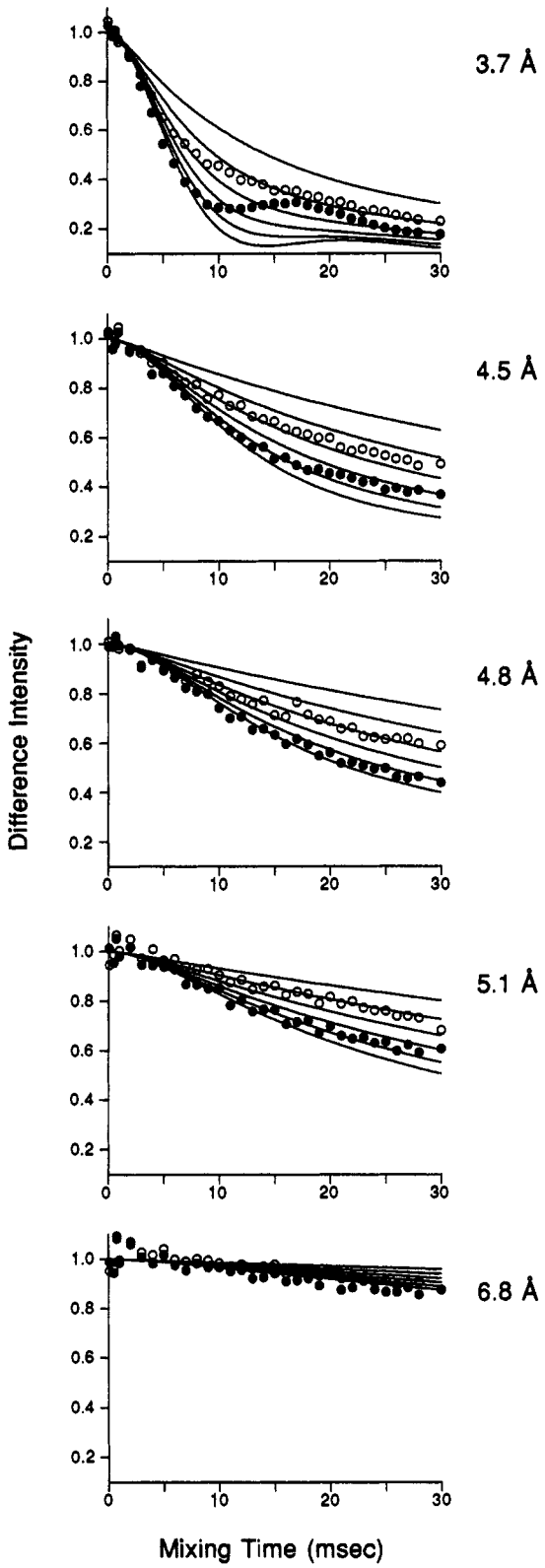

Figure 8. Comparison of the five sets of RR data obtained with 62 (○) and 83 kHz (●) proton decoupling with simulations using T_2^{ZQ} values from 1.0 (slow exchange rate) to 3.5 ms (fast exchange rate) in 0.5-ms steps. The other parameters for the calculations are given in Table 1.

slow exchange rates make it impossible to obtain statistically significant T_2^{ZQ} values because errors in normalizing the initial difference intensity to 1.0 become significant when compared to the low exchange rate and the additional modulation of the exchange rate by zero-quantum relaxation is quite small and within the scatter of the experimental data (Figure 6A). Even though unique T_2^{ZQ} values cannot be obtained from these data, it is interesting to note that the optimal fits to the two data sets require T_2^{ZQ} values that differ by ~1.5 ms, just as do the values determined for the shorter distances.

Estimating the Zero-Quantum T_2 Line Widths. Based on the work of Kubo and McDowell,[15] Griffin and co-workers have argued that the zero-quantum relaxation times required to simulate RR data, and thus estimate internuclear distances, can be obtained *directly* from the observed spectral line widths after correcting for magnetic field inhomogeneities.[16] The expression derived from the work by Kubo and McDowell states that the zero-quantum relaxation rate of an I··S homonuclear spin pair can be approximated from the single quantum relaxation time (T_2) of the two spins by the expression

$$1/T_2^{ZQ} = 1/T_2^{I} + 1/T_2^{S} \quad \text{or} \quad T_2^{ZQ} = 1/\pi(\nu^{I} + \nu^{S})$$

which can be written in terms of the full width at half maximum line widths (ν, in units of Hz) of the two resonances.

The measured line widths do not necessarily yield the true T_2 relaxation rates of the spins because they only represent the directly observable T_2*. The ^{13}C line widths observed in the natural abundance difference spectra (Figure 2) are significantly broader than expected from CP-MAS spectra of the individual amino acids; the carbonyl and methyl resonances in the five crystalline peptides have average line widths of 80.9 and 35.8 Hz, respectively, as compared to the 32 and 43 Hz line widths found for the alanine carboxyl and methyl resonances at 9 kHz MAS with 83 kHz proton decoupling. The origin of the larger peptide carbonyl line widths is most likely conformational heterogeneity in the sample which leads to a dispersion in the isotropic chemical shift; the 55-Hz discrepancy between the peptide and model compound line widths can be explained by a distribution of only ±0.014 Å in the backbone hydrogen bonding length.[17,18] Smaller line broadening effects also arise from a number of other sources, including spinning speed instabilities, local molecular motions, and magnetic susceptibilities.[19] The B_0 magnetic field inhomogeneity is about 0.05 ppm based on the ^{13}C line widths observed for adamantane and will account for at most ~5 Hz line broadening.

Table 4 compares the T_2^{ZQ} values needed to fit the RR data with values calculated using line widths obtained from several different sources. The line widths obtained from alanine, the free amino acid, at 9 kHz, correspond to a T_2^{ZQ} of 4.2 ms. These relatively small line widths are much less inhomogeneously broadened than those observed for alanine incorporated into the crystalline peptides (and thus represent an absolute lower limit

(16) Raleigh, D. P.; Creuzet, F.; Das Gupta, S. K.; Levitt, M. H.; Griffin, R. G. *J. Am. Chem. Soc.* **1989**, *111*, 4502. Spencer, R. G. S.; Halverson, K. J.; Auger, M.; McDermott, A. E.; Griffin, R. G.; Lansbury, P. T., Jr. *Biochemistry* **1991**, *30*, 10382. Thompson, L. K.; McDermott, A.; Raap, J.; van der Wielen, C. M.; Lugtenburg, J.; Herzfeld, J.; Griffin, R. G. *Biochemistry* **1992**, *31*, 7931. McDermott, A. E.; Creuzet, F.; Gebhard, R.; van der Hoef, K.; Levitt, M. H.; Herzfeld, J.; Griffin, R. G. *Biochemistry* **1994**, *33*, 6129.

(17) Saito, H. *Magn. Reson. Chem.* **1986**, *24*, 835. Saitô has investigated the conformation dependence of the ^{13}C chemical shift observed in solid-state CP-MAS NMR experiments and found a variation in the alanine carbonyl and methyl isotropic chemical shifts of 0.6 ppm (54 Hz) when the residues are located in α-helices. Ando and co-workers (ref 18) have also noted that the alanine carbonyl isotropic chemical shift is sensitive to the C=O··H−N hydrogen bond length with a slope of −21.7 ppm/Å and have modeled this effect with quantum mechanical methods by considering changes in the σ_{22} element of the chemical shift tensor, which lies along the C=O bond.

(18) Asakawa, N.; Kuroki, S.; Kurosu, H.; Ando, I.; Shoji, A.; Ozaki, T. *J. Am. Chem. Soc.* **1992**, *114*, 3261. Ando, S.; Ando, I.; Shoji, A.; Ozaki, T. *J. Am. Chem. Soc.* **1988**, *110*, 3380.

(19) VanderHart, D. L.; Earl, W. L.; Garroway, A. N. *J. Magn. Reson.* **1981**, *44*, 361.

Table 4. Comparison of Zero-Quantum Relaxation Times Obtained from Simulations with Those Calculated from Observed Line Widths[a]

source	line widths (Hz) $^{13}C{=}O$	line widths (Hz) $^{13}CH_3$	T_2^{ZQ} (ms)
simulations			3.0–3.5
alanine			
9 kHz MAS	32 Hz	43 Hz	4.2
14.5 kHz MAS	36	66	3.1
crystalline peptides			
9 kHz MAS	81	36	2.7
transverse T_2 measurements	50	40	3.5

[a] The experimental data were obtained with 83 kHz proton decoupling field strengths.

for the line widths that might be used for the simulations). Increasing the spinning speed to 14.5 kHz leads to broadening of the alanine resonances due to less efficient proton decoupling.[20] The broadening is more pronounced on the $^{13}CH_3$ line width due to its directly bonded protons. The line widths observed in the 14.5 kHz alanine spectrum correspond to a T_2^{ZQ} within the 3.0–3.5-ms range needed to fit the 83 kHz proton decoupling data.

In the case of the crystalline peptides, the average line widths observed in the 9-kHz difference spectra (Figure 2) correspond to a 2.7-ms T_2^{ZQ}. Comparison of these line widths with those of alanine suggests that the resonances are inhomogeneously broadened. A direct measurement of the homogeneous contribution to the observed line widths can be made with a transverse T_2 experiment.[21] Measurement of the homogeneous line widths for the crystalline peptides under static or MAS conditions yields values of ~50 and 40 Hz for the C=O and CH_3 resonances, respectively. These line widths correspond to a T_2^{ZQ} of 3.5 ms which is within the range needed to optimally fit the exchange data. Of importance is that these measurements clearly show that the C=O line width is much more inhomogeneously broadened than the CH_3 line width, in accord with the slight differences in hydrogen bonding.[16,17] It is apparent that inhomogeneous broadening occurs even in peptide crystals and that its effects should be taken into account (see below).

Dipolar Oscillations in the Magnetization Exchange Curves and Inhomogeneous Broadening. Generally, when the dipolar coupling is larger than the zero-quantum relaxation rate, $D > (T_2^{ZQ})^{-1}$, oscillations will be present at the $n = 1$ RR condition (e.g. which is the situation for directly bonded atoms) as the Zeeman magnetization moves from one spin population to the other and back again. The positions of the minima and maxima of these oscillations can be used to determine the internuclear distance without accurate knowledge of the zero-quantum relaxation time,[1] as is the case for the 3.7 Å spin pair peptide. As the internuclear distance is increased, the dipolar coupling decreases rapidly and the oscillations in the magnetization exchange curves become less pronounced and occur at later mixing times. When the dipolar coupling is much less than the zero-quantum relaxation rate, $D \ll (T_2^{ZQ})^{-1}$, the RR exchange curves exhibit a simple monotonic decay; the oscillations are prevented by relatively rapid relaxation of zero-quantum coherence. This behavior is displayed in the spectra of the 4.5, 4.8, 5.1, and 6.8 Å spin pair peptides. In this case it is not possible to independently determine the strength of the dipolar coupling and the zero-quantum relaxation time from the RR exchange data because changing either T_2^{ZQ} or D has the same effect on the calculated exchange curve. Consequently, the appropriate T_2^{ZQ} value must be known independently if one seeks to determine the internuclear distance with a RR experiment. Unfortunately, many applications will fall into this second regime and an accurate method for estimating the zero-quantum relaxation time is thus essential for determining the dipolar coupling with simulations. However, it is difficult to experimentally measure the T_2^{ZQ}.

Although the qualitative agreement between the observed and calculated curves is quite good for the 4.5, 4.8, 5.1, and 6.8 Å spin pairs (Figure 8), the data from the 3.7 Å spin pair show that simulation of the experimental results is not straightforward. The calculated curves for 3.7-Å peptide overestimate both the position of the oscillation and the amount of magnetization exchange at the later time points.

The reduction in the observed magnetization exchange may arise from several sources. Most obvious is underestimating the natural abundance ^{13}C background signals, which reduces the apparent RR exchange rate because the exchange curve is improperly normalized. Along the same lines, reduced incorporation efficiency of ^{13}C labeled at one of the sites in the exchanging pair leads to a situation where there are *singly* labeled molecules that cannot participate in RR exchange because the second member of the spin pair is a magnetically silent ^{12}C atom. Incomplete excitation or inversion of the carbonyl spins will also reduce the apparent exchange rate because the ensemble Zeeman population difference within the $^{13}C\cdots{}^{13}C$ pairs is non-zero at the start of the mixing period. The net magnetization difference after complete exchange then becomes some positive value. The calculations assume an initial state of equal but opposite spin populations within the exchanging pair that can be difficult to achieve in practice; if the cross-polarization rates of the two spins are not comparable or if the spins differ in their rotating frame relaxation rates ($T_{1\rho}$) it may be impossible to generate equal initial spin populations within the exchanging pair. These effects are compounded by the fact that the dipolar coupling between the spins is "on" during the CP and selective inversion pulses because the sample is spinning at RR. For strong dipolar coupling, this can lead to exchange of magnetization even before the RR mixing period is started. Such pre-exchange will affect the final value of the RR exchange curve because it is being normalized incorrectly.

The position of the oscillation, on the other hand, is solely determined by the dipolar coupling and the position observed corresponds to a distance of 3.5 Å; this indicates an error of 0.2 Å in the accuracy of the RR experiment based on the 3.7-Å distance observed in the peptide crystal structure. This may well be caused by inhomogeneous broadening due to conformational heterogeneity in the sample, which results in some of the dipole-coupled spin pairs not being on rotational resonance.

Figure 9 presents a set of simulations as a function of the MAS frequency offset from rotational resonance. The lowest curve is on rotational resonance and each subsequent curve is progressively 40 Hz off rotational resonance. The 40 Hz offset approximates the homogeneous line width. The simulations show that increasing the offset from rotational resonance results in loss of magnetization exchange along with a shift in the dipolar oscillation to shorter mixing times. This is the behavior observed in the 3.7-Å peptide and provides an explanation for the discrepancy discussed above between the observed exchange curve and the simulations. These results indicate that inhomogeneous broadening is important in any analysis of RR magnetization exchange curves and contributes to the error in the measurements on these peptide crystals of at most 0.2 Å.

(20) Peersen, O. B.; Smith, S. O. *Concepts Magn. Reson.* **1993**, *5*, 303.
(21) Garroway, A. N. *J. Magn. Reson.* **1977**, *28*, 365. Smith, S. O.; Hamilton, J.; Salmon, A.; Bormann, B. J. *Biochemistry* **1994**, *33*, 6327.

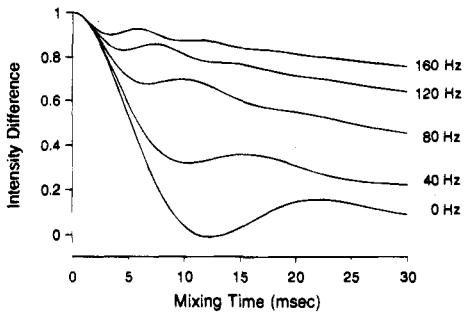

Figure 9. Comparison of magnetization exchange simulations on and off rotational resonance. The exchange curve on rotational resonance (bottom curve) exhibits rapid magnetization exchange. As the MAS frequency is increased in increments of 40 Hz, the magnetization exchange curves become damped and the dipolar oscillations shift to shorter mixing times. The simulations are based on the parameters for the 3.7-Å peptide with a 6.0-ms T_2^{ZQ}.

Conclusions

The overall conclusion from the RR NMR experiments presented in this study is that the method does have the range and resolution necessary to make measurements on the local secondary structure and tertiary packing of membrane proteins. Significant and interpretable ^{13}C RR magnetization exchange rates can be observed for internuclear distances up to 6−6.5 Å with an experimental resolution of ~0.1 Å. Although this distance range applies to $^{13}C\cdots{}^{13}C$ experiments in general, it is important to realize that the resolution is mainly a measure of the experimental precision and that the resolution will be highest in well-defined peptide crystals. The accuracy in the measurement of an unknown distance is lower because many other factors affect the magnetization exchange curves.

The two greatest contributors to the error are the corrections for natural abundance background signals and the effects of the proton decoupling field strength. Background signals must be carefully accounted for because the presence of unchanging background intensity will reduce the apparent RR exchange rate and lead to an overestimate of the internuclear distance. The proton decoupling field strength acts directly on the rate of magnetization exchange, which is reduced in the presence of insufficient decoupling. In calculations of RR exchange curves, the decoupling dependence is properly accounted for by the zero-quantum relaxation time and T_2^{ZQ} values of 1.5−2.0 and 3.0−3.5 ms are needed to reproduce the experimental data obtained with 62 and 83 kHz decoupling fields.

It should be reemphasized that since the proton decoupling strength is generally not uniform across the sample due to inhomogeneity in the B_1 field strengths, the zero-quantum relaxation rate is also not uniform and for a given $^{13}C\cdots{}^{13}C$ pair it will then depend on where in the sample coil the spin pair is located. The result is that $^{13}C\cdots{}^{13}C$ spin pairs with identical internuclear distances will have different RR exchange rates solely because of their location in the sample coil. In the case of large sample volumes and relatively weak proton decoupling fields, it is not correct to model the RR data using a single T_2^{ZQ} value, but rather the RR data should be calculated with a weighted average of several T_2^{ZQ} values corresponding to RR exchange in different parts of the sample rotor.

Our model peptide system has been essential in establishing the experimental accuracy of the RR determined distances. In this system, reducing the proton decoupling strength from 83 to 62 kHz causes the exchange rate to decrease by an amount corresponding to ~0.3 Å in internuclear distance. Assuming that in a general case one can easily calibrate the decoupling strength to within ±5 kHz of the desired value and that B_1 field inhomogeneity effects are comparable to those in the 5-mm probe used here, then decoupling effects alone will only diminish the accuracy of RR determined distances by ~±0.1 Å. A larger error, however, results from inaccurately accounting for background signals. In the crystalline model peptide the natural abundance ^{13}C background signals could be accounted for with an error of only 2−3%, resulting in a distance error in the final exchange curves that is comparable to the one arising from the proton decoupling effects. Together, these two sources of error indicate that the accuracy in the NMR distance determinations for the crystalline peptides is on the order of 0.2−0.3 Å. This estimate only pertains to the $n = 1$ RR data; the situation degrades rapidly for $n \geq 2$ data because the exchange rates become increasingly sensitive to the molecular geometry of the spin pair.

In the general case when one encounters significant background signals or weak NMR resonances, it is difficult to justify accounting for the errors with such accuracy. Given a ±5% error in establishing the initial points on the RR exchange curves, the error in the distance determination is on the order of ~±0.2 Å for distances in the 4−6-Å range. For many biological applications, where the signals are extremely weak and the RR difference spectra are considerably noisier than in Figures 1 and 2, a ±5% error would be considered low.

Given the large number of parameters that affect the RR exchange rates, how does one then interpret exchange curves in the general case? One feasible approach is to interpret RR data only in terms of upper and lower limits on the internuclear distance. An upper limit on the distance can be obtained by simulating the data with a T_2^{ZQ} determined from line widths observed in MAS spectra obtained near the RR condition. Fitting the maximum observed line width provides a lower limit on the T_2 values of the two spins and thus a lower limit on the T_2^{ZQ}. Simulations with this zero-quantum relaxation value represent the slowest possible exchange rates and a comparison with the data will give an upper estimate of the distance. Conversely, a lower limit on the distance can be obtained by simulating the data with a T_2^{ZQ} determined from line widths obtained from crystalline model compounds. The minimum line widths are observed in the crystalline model compounds because there is little or no conformational heterogeneity in the sample. Based on the results above, the distance derived from simulations using the model compound line widths will be more accurate than those estimated using the observed inhomogeneously broadened line widths. The advantage of this approach is that these line widths and the corresponding limits are easy to measure and serve to bracket the actual distance.

Alternatively, RR data can be interpreted by comparisons with standard (e.g. crystal) curves as we have shown previously. In this case, the standard and unknown data sets should involve identical types of $^{13}C\cdots{}^{13}C$ spin pairs; this provides to a first approximation identical $^{13}C\cdots{}^{1}H$ and $^{1}H\cdots{}^{1}H$ couplings. The two sets of experiments should be performed with the same proton decoupling field strengths and in the same type of sample coil so that effects from inhomogeneous B_1 fields are correlated. The advantage of this approach is that it provides a direct estimate of an unknown internuclear distance without resorting to simulations.

It is important to emphasize that in general inhomogeneous broadening of the observed NMR line widths is much more substantial in noncrystalline peptides and proteins. In cases where inhomogeneous broadening is significant, it is possible to estimate the homogeneous line width in a transverse T_2 experiment.[21] In these situations, one must simulate both the on- and off-RR contributions to the magnetization exchange

curves. The experimental accuracy of the method under these conditions, however, may be hard to quantitate since the large inhomogeneous line width may reflect a *distribution* of distances between the dipole-coupled spins in the sample.

In summary, rotational resonance NMR methods provide the means to measure internuclear distances in magic-angle spinning experiments. We have outlined the experimental setup for these experiments and discussed many of the issues that bear on translation of RR magnetization exchange curves into accurate distances. An analysis of the magnetization exchange curves from the set of crystalline peptides in this study shows that the accuracy of the distance measurements depends on the precision of the measurements as well as correctly accounting for natural abundance background signals, the effects of proton B_1 field strengths, and inhomogeneous broadening of the dipole-coupled NMR resonances.

Acknowledgment. This research was supported by grants from National Institutes of Health (GM 41412 and GM 46732) and the Department of the Army (DAMD 17-94-J-4048). We thank Malcolm Levitt for an updated version of the CC2Z simulation program and Günther Metz and Andrew Kolbert for helpful discussions.

JA9502637